Макрогетероциклы
http://mhc-isuct.ru

DOI: 10.6060/mhc245865m

(5,10,15,20-Tetra(4-trifluoromethylphenyl)porphinato)cobalt(II). Reactions with Heterocyclic Bases as the Model for the Donor-Acceptor PET Systems Formation

Elena V. Motorina,[a@] Tatyana N. Lomova,[a] and Irina A. Klimova[a,b]

[a]*G. A. Krestov Institute of Solution Chemistry of the Russian Academy of Sciences, 153045 Ivanovo, Russian Federation*
[b]*Ivanovo State University of Chemistry and Technology, 153000 Ivanovo, Russian Federation*
[@]*Corresponding author E-mail: evm@isc-ras.ru*

This study was carried out taking into account the need to find the optimal nature of the anchor group when creating coordination-type PET systems based on metalloporphyrins and carbon nanoform derivatives and to find the key characteristics of the first ones as receptors of heterocyclic bases in sensory. The equilibriums and rates of reactions of (5,10,15,20-tetra(4-trifluoromethylphenyl)porphinato)cobalt(II) (CoT(4-CF_3Ph)P) with pyridine and imidazole (Py and Im) in toluene were studied by the time-dependent spectrophotometric titration, designed specifically for slowly settling equilibriums. To confirm the chemical structure of the resulting complexes the methods of electronic and IR absorption spectroscopy, ^{1}H NMR and mass spectrometry were used. Fast and slow coordination of the first and the second base molecule, respectively, was established, occurring in both cases reversibly. The coordination equilibrium constants K_1, K_2 are determined to be $3.16\cdot10^3$, $1.53\cdot10^3$ and $1.12\cdot10^4$, $4.28\cdot10^3$ L·mol^{-1} for Py and Im, respectively. Im molecules coordinated faster compared to Py ($k=1.033$ and $56.1\cdot10^{-4}$ L·mol^{-1}·s^{-1}) are more strongly bonded by the porphyrin complex and demonstrate practically more acceptable values of the optical response and the minimum limit of base determination. These parameters must be taken into account when forming metalloporphyrin–substituted fulleropyrrolidine coordination complexes along with the reversibility of the process, the required distance between the donor and acceptor, and the lifetime of PET states upon photoexcitation.

Keywords: Cobalt porphyrin, pyridine, imidazole, coordination complexes, chemical structure, formation parameters, spectroscopy.

(5,10,15,20-Тетра(4-трифторметилфенил)порфинато)кобальт(II). Реакции с гетероциклическими основаниями как модель формирования донорно-акцепторных PET систем

Е. В. Моторина,[a@] Т. Н. Ломова,[a] И. А. Климова[a,b]

[a]*Институт химии растворов им. Г.А. Крестова Российской академии наук, 153045 Иваново, Российская Федерация*
[b]*Ивановский государственный химико-технологический университет, 153000 Иваново, Российская Федерация*
[@]*E-mail: evm@isc-ras.ru*

Данное исследование проведено с учетом необходимости нахождения оптимальной природы якорной группы при создании PET систем координационного типа на основе металлопорфиринов и производных наноформ углерода и для нахождения ключевых характеристик первых как рецепторов гетероциклических оснований в сенсорике. Изучены равновесия и скорости реакций (5,10,15,20-тетра(4-трифторметилфенил)порфинато)-кобальта(II) (CoT(4-CF_3Ph)P) с имидазолом и пиридином (Im и Py) в среде толуола методом время-зависимого спектрофотометрического титрования, разработанного специально для медленно устанавливающихся равновесий. Для доказательства химического строения образующихся комплексов использованы методы электронной и ИК спектроскопии поглощения, ^{1}H ЯМР и масс-спектрометрии. Установлена быстрая и медленная координация соответственно первой и второй молекулы оснований, протекающая в обоих случаях обратимо. Константы равновесий координации K_1, K_2 определены равными $3.16\cdot10^3$, $1.53\cdot10^3$ и

$1.12 \cdot 10^4$, $4.28 \cdot 10^3$ л·моль$^{-1}$ для Py и Im соответственно. Молекулы Im, координируюясь быстрее по сравнению с Py (k = 1.033 и $56.1 \cdot 10^{-4}$ л·моль$^{-1}$·с$^{-1}$), сильнее связываются порфириновым комплексом и демонстрируют практически более приемлемые значения оптического отклика и минимального предела определения основания. Эти параметры необходимо учитывать при формировании координационных комплексов металлопорфирин – замещенный фуллеропирролидин наряду с учетом обратимости процесса, требуемого расстояния между донором и акцептором и времени жизни PET состояний при фотовозбуждении.

Ключевые слова: Порфиринат кобальта, пиридин, имидазол, координационные комплексы, химическое строение, параметры образования, спектроскопия.

Introduction

Metalloporphyrins (MPs) that are being intensively studied are promising compounds for practical applications due to their highly specific nature. The axial coordination characteristic of metalloporphyrins plays important role in the oxidation processes of organic compounds, donor-acceptor complex formation, homogeneous and heterogeneous catalysis, and dissociation reactions.[1–17] To date, it has been established that complexes with metals of variable valence, especially with cobalt, exhibit the greatest reactivity. The nature of the axial coordination to the cobalt complexes with macrocyclic ligands is widely studied, including with the aim of using them as the synthetic analogs of the natural oxygen carriers cyanocobalamin and coboglobin.[18] A number of cobalt complexes with the Schiff bases have been synthesized and the facilitated transport of molecular oxygen in the polymer membranes containing these complexes as oxygen carriers has been studied.[19] The review[20] focuses on the recent advances in the use of natural cobalamins and their synthetic analogs in medical practice as the vectors for the targeted delivery of drugs to tumors. The influence of peripheral substituents and axial ligands (Py, Im, THF, CO) on the electronic structure and the properties of the cobalt tetraphenylporphyrin complex (CoTPP) was studied using DFT methods.[21] The preparation of cobalt-porphyrin-polypyridyl surface coatings for photoelectrosynthesis of hydrogen was confirmed by spectroscopic methods.[22] The reactivity of a number of cobalt porphyrins with the π-extending or strongly electron-withdrawing β-pyrrole substituents in non-aqueous media was studied.[23]

The data on the thermodynamics and kinetics of coordination reactions of volatile organic compounds (VOCs), small organic molecules and fullerene-containing N-bases with porphyrin complexes which demonstrate the wide range of the changes in chemical and physical properties depending on the nature of the macrocycle/the central metal atom/axial ligands (if any) have been to date obtained.[24–31] Based on porphyrin complexes of cobalt(II) and fulleropyrrolidines, which act as an electron donor and an electron acceptor, respectively, systems with the property of the photoinduced electron transfer (PET)[32–35] and the molecular complexes with the N heterocyclic bases of varying structures have been obtained.[36,37] A huge number of synthetic drugs are heterocyclic compounds. For example, pyridine and imidazole derivatives are used for the synthesis of antimicrobial, antihistamine, antipyretic drugs and are biologically active compounds with a wide spectrum of action. The ability of many heterocycles to form the strong complexes with metals, which is applicable for the targeted drug delivery and the development of chemical sensors and antidotes, is of important biochemical significance.[38,39]

Graphene and its derivatives, carbon nanotubes, as well as carbon dots and carbon nanohoops involving non-covalent coupling to porphyrins display photophysics which allow for the use of these materials in biomedical and environmental applications with the emphasis on imaging, biosensing, and the delivery of drugs in nanomedicine.[40] The carbon nanoforms and porphyrins can act in some of these applications as an electron acceptor and an electron donor. One of the common methods for obtaining the PET systems with the acceptor part of the fullerene nature is bonding of the fullerene frame on the central metal atom through the substituent heteroatom in fulleropyrrolidine. Therefore, the study of MP reactions with heterocyclic bases that are usually used to search for suitable sensors for these bases, takes on a new meaning consisting in the need to find the optimal nature of the anchor group when creating the coordination-type PET systems.

In this work, the equilibriums and rates of reactions of (5,10,15,20-tetra(4-trifluoromethylphenyl)porphinato)cobalt(II) (CoT(4-CF_3Ph)P, Figure 1) with pyridine and imidazole (Py and Im) in toluene were studied using the time-dependent spectrophotometric titration method developed specifically for slowly established equilibriums.[41] To establish the chemical structure of the resulting complexes, the data of spectral methods were used (UV-Vis, IR, ^{1}H NMR, and MS (MALDI-TOF)). The studied reactions are the model for the self-assembly of the donor-acceptor systems based on metalloporphyrins and the derivatives of carbon nanoforms. The study of the ones allows us to determine the key parameters of CoT(4-CF_3Ph)P as the receptor for the N-heterocyclic bases.

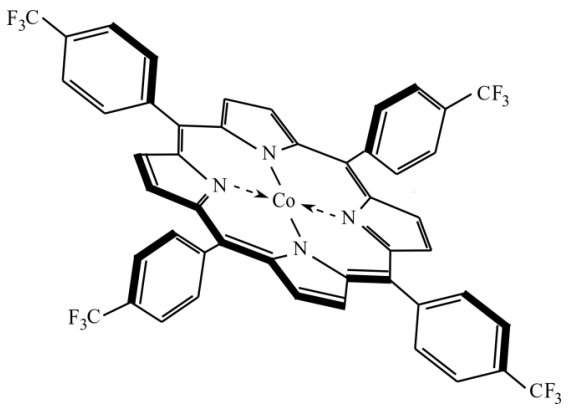

Figure 1. The chemical structure of (5,10,15,20-tetra(4-trifluoromethylphenyl)porphinato)cobalt(II).

Experimental

Synthesis

(5,10,15,20-Tetra(4-trifluoromethylphenyl)porphinato)cobalt(II), CoT(4-CF_3Ph)P (**1**) was synthesized by reaction of (0.02 g, $2.25\cdot10^{-5}$ mol) H_2T(4-CF_3Ph)P with $Co(AcO)_2\times4H_2O$ (0.028 g, $1.12\cdot10^{-4}$ mol) in boiling dimethylformamide (DMF) for 10 min. The contents of the reaction flask were cooled, diluted with water and the products were extracted into chloroform. The solution in $CHCl_3$ was repeatedly washed with distilled water to remove DMF. $CHCl_3$ was partially distilled off. The residual solution was purified by the chromatography on the Al_2O_3 column (grade II activity according to Brockman) using chloroform. The yield is 79%. UV–Vis (toluene) λ_{max} (log ε) nm: 413 (5.44), 528 (4.41), 613 (4.02). IR (KBr) ν cm^{-1}: vibrations of benzene rings 686, 717 (γ C–H), 1069, 1167 (δ C–H), 3046, 3067 (ν C–H), 1546, 1574, 1617 (ν C=C); vibrations of pyrrole rings 798 (γ C–H), 1003 (C_3–C_4, ν C–N, δ C–H), 1328 (ν C–N), 1458 (ν C=N); 1106, 1125, 1247 (ν C–F); 442 (Co–N). ^{1}H NMR ($CDCl_3$) δ ppm: 15.71 (br. s, $8H_\beta$), 13.10 (br. s, $8H_o$), 10.18 (s, $8H_m$). MALDI-TOF (CHCA) *m/z*: found 943.89 $[M]^+$; calculated for $C_{48}N_4H_{24}F_{12}Co$ 943.66.

(5,10,15,20-Tetra(4-trifluoromethylphenyl)porphinato)di(pyridine)cobalt(II), Co(Py)$_2$T(4-CF_3Ph)P (**2**), was synthesized by the reaction of CoT(4-CF_3Ph)P with Py in the molar ratio of 1: 2 in toluene at 298 K for a month. The solid complex was crystallized from the toluene solution. The yield is approximately 100%. UV–Vis (toluene) λ_{max} nm: 438, 555. IR (KBr) ν cm^{-1}: vibrations of benzene rings 684, 700 (γ C–H), 1068, 1168 (δ C–H), 3045, 3071 (ν C–H), 1536, 1574, 1617 (ν C=C); vibrations of pyrrole rings 794 (γ C–H), 1010 (C_3–C_4, ν C–N, δ C–H), 1324 (ν C–N), 1447 (ν C=N); 1108, 1126, 1211 (ν C–F); 438 (Co–N). ^{1}H NMR ($CDCl_3$) δ ppm: 14.12 (br. s, $8H_\beta$), 11.01 (br. s, $8H_o$), 9.43 (s, $8H_m$) 7.95 (br. m, $6H_{o,p}$, Py), solvent residual signal region 7.26 (br. s, $4H_m$, Py). MALDI-TOF (DHB) *m/z*: 944.43 $[M\text{-}2Py]^+$; calculated for $C_{48}N_4H_{24}F_{12}Co$ 943.66, 1114.10 $[M\text{-}2Py+DHB]^+$; calculated for $C_{48}N_4H_{24}F_{12}Co$+DHB 1097.78. MALDI-TOF (CHCA) *m/z*: 943.45 $[M\text{-}2Py]^+$; calculated for $C_{48}N_4H_{24}F_{12}Co$ 943.66, 1132.34 $[M\text{-}2Py+CHCA]^+$; calculated for $C_{48}N_4H_{24}F_{12}Co$+CHCA 1132.88. MALDI-TOF (without matrix) *m/z*: 943.27 $[M\text{-}2Py]^+$; calculated for $C_{48}N_4H_{24}F_{12}Co$ 943.66.

(5,10,15,20-Tetra(4-trifluoromethylphenyl)porphinato)di(imidazole)cobalt(II), Co(Im)$_2$T(4-CF_3Ph)P (**3**), was synthesized by the reaction of CoT(4-CF_3Ph)P with Im in the molar ratio of 1: 2 in toluene at 298 K for a day. The solid complex was crystallized from the toluene solution. The yield is approximately 100%. UV–Vis (toluene) λ_{max} nm: 434, 552. IR (KBr) ν cm^{-1}: vibrations of benzene rings 739, 759 (γ C–H), 1056, 1149 (δ C–H), 3016, 3124 (ν C–H), 1498, 1543, 1577 (ν C=C); vibrations of pyrrole rings 828 (γ C–H), 937 (C_3–C_4, ν C–N, δ C–H), 1328 (ν C–N), 1449 (ν C=N); 1102, 1244 (ν C–F); 441 (Co–N). ^{1}H NMR ($CDCl_3$) δ ppm: 8.69 (s, $8H_\beta$), 8.37 (br. s, $8H_o$), 7.63 (s, $8H_m$), 7.46 (d, $2H_{Im(2)}$), 7.81 (t, $2H_{Im(NH)}$), 7.07 (s, $4H_{Im(4,5)}$). MALDI-TOF (DHB) *m/z*: 944.08 $[M\text{-}2Im]^+$; calculated for $C_{48}N_4H_{24}F_{12}Co$ 943.66, 1094.04 $[M\text{-}2Im+DHB]^+$; calculated for $C_{48}N_4H_{24}F_{12}Co$+DHB 1097.78. MALDI-TOF (CHCA) *m/z*: 944.14 $[M\text{-}2Im]^+$; calculated for $C_{48}N_4H_{24}F_{12}Co$ 943.66, 1132.70 $[M\text{-}2Im+CHCA]^+$; calculated for $C_{48}N_4H_{24}F_{12}Co$+CHCA 1132.88. MALDI-TOF (without matrix) *m/z*: 944.01 $[M\text{-}2Im]^+$; calculated for $C_{48}N_4H_{24}F_{12}Co$ 943.66.

All reagents were of analytical grade. Chloroform, DMF, toluene, and imidazole were purchased from Acros Organics. H_2T(4-CF_3Ph)P was received from PorphyChem.

Time-dependent spectrophotometric titration

The equilibriums and the rates of the reactions between CoT(4-CF_3Ph)P and organic bases were spectrophotometrically studied in toluene by the molar ratio and the excess concentration method, respectively. The solutions of CoT(4-CF_3Ph)P, Py, and Im in toluene were prepared immediately before use to avoid the formation of peroxides in the solvent medium. The absorbance of the solutions with both the constant CoT(4-CF_3Ph)P concentration of $4.95\cdot10^{-6}$ and $5.12\cdot10^{-6}$ M for the reaction with Py and Im, respectively, and the increasing base concentration was measured at the working wavelength of 412 nm at the initial moment of time (τ = 0) and during the reaction until its end (τ = ∞). The concentration of Py and Im was changed from zero to 9.93 $mol\cdot L^{-1}$ and from zero to $3.33\cdot10^{-3}$ $mol\cdot L^{-1}$, respectively. The solutions were thermostatted with the error of ± 0.1 K at 298 K in the closed quartz cells placed in a spectrophotometer camera. Spectrophotometric titration data in the concentration and time fields (time-dependent spectrophotometric titration method[38]) were used to determine the equilibrium constants (Equation 1), the rates of one-way reactions (Equation 2), and equilibration time (from the minimum error in the numerical value of the equilibrium constant calculated at different τ values) in one experimental series.

Equation (1) was derived for the mixture of two colored compounds, initial CoT(4-CF_3Ph)P and the product of its reaction with Py/Im, using the law of mass action and the Bouguer–Lambert–Beer law.

$$K = \frac{(A_i - A_0)/(A_\infty - A_0)}{1-(A_i - A_0)/(A_\infty - A_0)} \cdot \frac{1}{(C_L^0 - C_{CoP}^0 \cdot (A_i - A_0)/(A_\infty - A_0))^m} \quad (1)$$

Here, C^0_{CoP} and C^0_L is the initial concentration of CoT(4-CF_3Ph)P and the one of Py/Im, respectively, in toluene. A_0, A_i and A_∞ is the absorbance at the working wavelength for the CoT(4-CF_3Ph)P solution at τ = 0 or τ = ∞, for that of an equilibrium mixture at a definite Py/Im concentration, and for a reaction product in a solution, respectively; *m* is the number of Py/Im molecules involved in the reaction.

The rate constants k_2 were observed using the dependence $\log k_{obs} - f(\log C_{Py/Im})$ where k_{obs} is the observed first order rate constant calculated by equation (2). The $k_{2\text{-}}$ values were calculated according to the law of acting masses: $k_{2\text{-}} = k_2/K_2$.

$$k_{obs} = \frac{1}{\tau} \ln \frac{A_0 - A_\infty}{A_\tau - A_\infty} \quad (2)$$

Here A_0, A_τ and A_∞ is the absorbance of a reaction mixture at a working wavelength at moments of the time 0, τ, and at the end of a reaction, respectively.

The methods of the chemical structure confirmation

The UV-Vis, IR, and ^{1}H NMR spectra were recorded on a UV-Vis Agilent 8453 spectrophotometer, a VERTEX 80v spectrometer, and an AVANCE-500 spectrometer, respectively. The mass spectra were performed on an Axima Confidence (Shimadzu Biotech, a 337-nm nitrogen laser) spectrometer with a time-of-flight mass analyzer by recording the spectra in the positive-ion mode. To record the ^{1}H NMR, mass and IR spectra of Co(Py)$_2$T(4-CF_3Ph)P and Co(Im)$_2$T(4-CF_3Ph)P, the equilibrium mixtures of the composition corresponding to the equivalence point on the titration curves of CoT(4-CF_3Ph)P with Py and Im were prepared. For NMR studies, the solvent was replaced with $CDCl_3$. To obtain a solid sample, when recording IR spectra in KBr, the solvent was evaporated.

Results and Discussion

N-bases taken act as σ-donor ligands with approximately the same field strength[21] and exhibit aromatic properties. Both compounds are the weak bases with basicity constants pK_b of 8.8 and 6.9 for Py and Im, respectively. The phenomenon of tautomerism, which allows both nitrogen atoms in Im to participate in the charge delocaliza-

tion[42], increases its basicity compared to Py. Py and Im when interacts with CoT(4-CF_3Ph)P change noticeably its highly specific UV-vis spectrum, which made it possible to study the Py/Im axial coordination reactions using the spectrophotometric method. The spectral response of CoT(4-CF_3Ph)P observed over time in the presence of the bases at the various concentrations shows that the coordination is not the one-step process and occurs as the complex reaction. Figure 2 shows the electronic spectra of CoT(4-CF_3Ph)P and its equilibrium mixtures with the bases at the initial time and at the end of all reactions in the solution.

With an increase in the concentration of N-bases in a wide range (Figure 2), the decrease in the intensity of the B(0,0) band (Soret band[43]) at $\tau = 0$ and its bathochromic shift from 413 to 438 and 434 nm for Py and Im, respectively, at $\tau = \infty$ is observed. The low-intensity Q(0,1) band in the visible region is shifted from 528 to 555 and 552 nm, respectively, for Py or Im. It can be observed in Figure 2 that the band at 528 nm, which belongs to the non-coordinated with the base CoT(4-CF_3Ph)P, is still present at $\tau = \infty$ in the spectrum of the equilibrium mixtures with Py at its low concentrations. The band of the reaction product with Im at 552 nm is already observed in the spectra of the equilibrium mixtures at high concentrations of Im. Study of the process in a time field in a specific narrower range of concentrations of both bases shows the absence of the CoT(4-CF_3Ph)P band at 528 nm in the spectra of the reaction products (Figures 3, 4). Thus, the reaction with Py and Im is displayed in the UV-vis spectrum as the quickly established equilibrium and the subsequent slow also reversible process, which partially overlap each other if we consider the entire wide range of the base concentrations. Despite this, the method of anatomizing chemical reactions (in this case, isolating the spectral curves in the series with the conserved isosbestic points) allows us to determine both equilibrium constants (fast and slow) with the acceptable accuracy (Experimental). The equilibrium constants of the CoT(4-CF_3Ph)P reactions with Py/Im were determined (Table 1). The *m* values observed from the data in Figures 5 and 6 is approximately 1 for the both the equilibrium sated at $\tau = 0$ and at $\tau = \infty$.

Judging by the found stoichiometry of fast equilibrium (Table 1), the pentacoordination complexes, Co(Py)T(4-CF_3Ph)P and Co(Im)T(4-CF_3P)P, are easily formed in the equilibrium mixtures in toluene at $\tau = 0$, which is favored by the asymmetrically filled outer shell of cobalt(II) d^7. The formation of six-coordinate complexes is difficult and occurs over time. There are cases when it was possible to determine only K_1 for the bonding of an axial ligand, for example, with the CoTPP or Co(T(4-OCH_3)PP) complexes.[18,36,44,46] However, K_2 values were obtained for cobalt(II) porphyrin complexes with electron-withdrawing peripheral substituents.[47,48] CoT(4-CF_3Ph)P studied in this work belongs to the last group of porphyrin complexes. The picture of the UV-Vis spectra transformation with distinct isosbestic points presented in Figures 2 and 3 is characteristic of the formation process for hexacoordination cobalt(II) complexes. The rate of the Co(Py)$_2$T(4-CF_3Ph)P or Co(Im)$_2$T(4-CF_3Ph)P formation depends on the base concentration. The spectrum changes very slowly in the range of low Py concentrations, and the reaction reaches equilibrium slowly (up to 1 month) at room temperature (Figure 3). The equilibrium in the system at high base concentrations is achieved within 24 hours (Figure 3d). Bonding of the second Im molecule by the Co(Im)T(4-CF_3Ph)P also occurs over time; the equilibrium in the system at the minimum C_{Im} of $7.24 \cdot 10^{-5}$ mol·L^{-1}and at the maximum C_{Im} of $3.33 \cdot 10^{-3}$ mol·L^{-1} is achieved within 4 hours and 1 hour, respectively. The reaction orders and the forward and reverse reaction rate constants for slow processes are represented in Table 1.

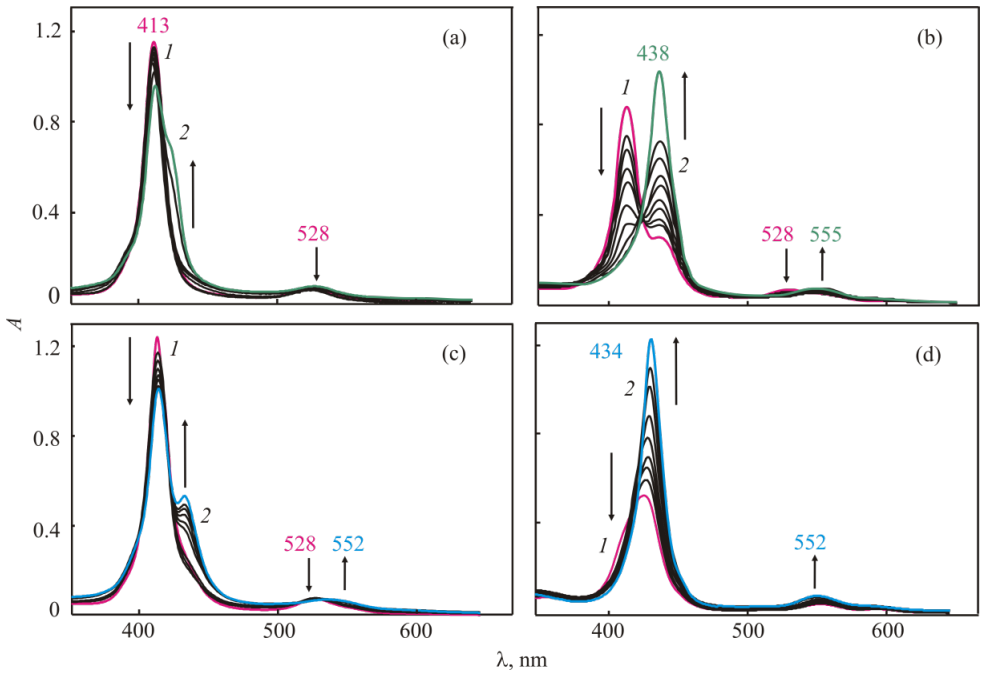

Figure 2. The UV-Vis spectra of CoT(4-CF_3Ph)P in toluene with the various base additives at $\tau = 0$: $C_{MP} = 4.95 \cdot 10^{-6}$ mol·L^{-1}, C_{Py} *1* – 0, *2* – 9.93 mol· L^{-1} (a); $C_{MP} = 5.12 \cdot 10^{-6}$ mol·L^{-1}, C_{Im} *1* – 0, *2* – $3.33 \cdot 10^{-3}$ mol· L^{-1} (c) and at $\tau = \infty$: $C_{MP} = 4.95 \cdot 10^{-6}$ mol· L^{-1}, $C_{Py} = 1$ – 0, *2* – 9.93 mol·L^{-1} (b); $C_{MP} = 5.12 \cdot 10^{-6}$ mol·L^{-1}, $C_{Im} = 1$ – 0, *2* – $3.33 \cdot 10^{-3}$ mol·L^{-1} (d). The remaining lines correspond to the intermediate concentrations of the bases.

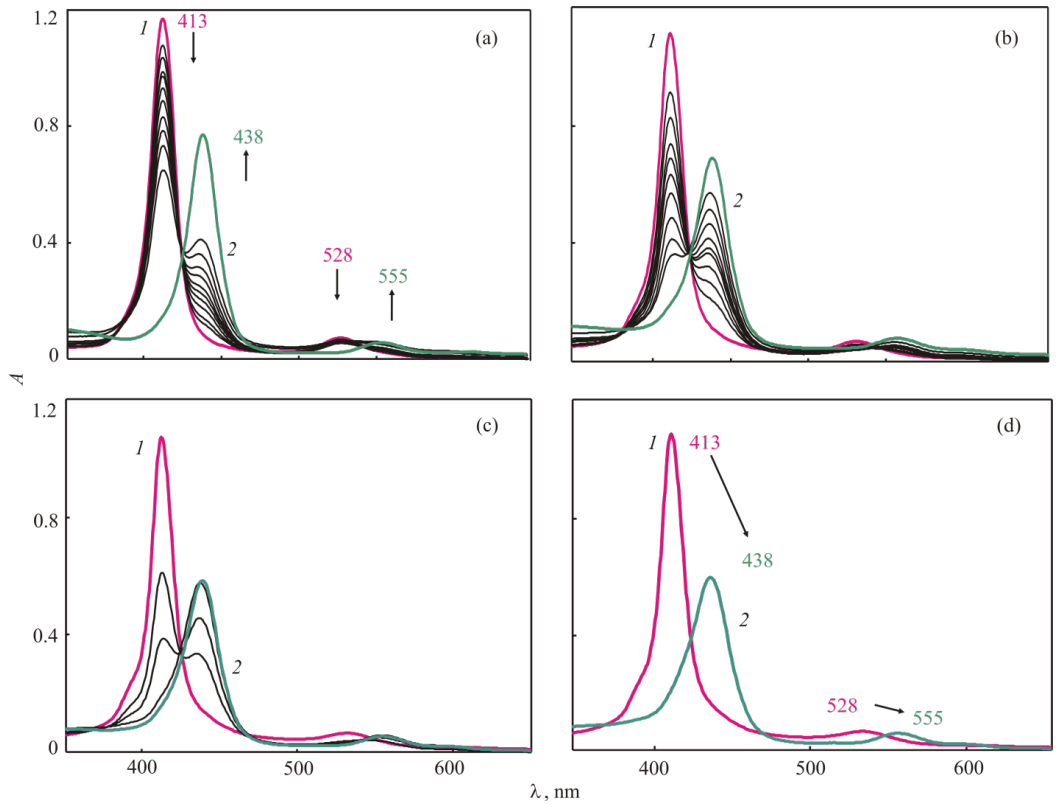

Figure 3. The UV-Vis spectra of CoT(4-CF_3Ph)P ($C = 4.95 \cdot 10^{-6}$ mol·L^{-1}) with the addition of Py: $C_{Py} = 5.95 \cdot 10^{-5}$ mol·L^{-1} at τ = 0 (*1*) and after a month (*2*) (a); $C_{Py} = 5.95 \cdot 10^{-4}$ mol·L^{-1} at τ = 0 (*1*) and after 25 days (*2*) (b); $C_{Py} = 9.92 \cdot 10^{-3}$ mol·L^{-1} at τ = 0 (*1*) and after 16 days (*2*) (c); $C_{Py} = 2.98 \cdot 10^{-2}$ mol·L^{-1} at τ = 0 (*1*) and after 24 h (*2*) (d). The remaining lines correspond to intermediate points in time.

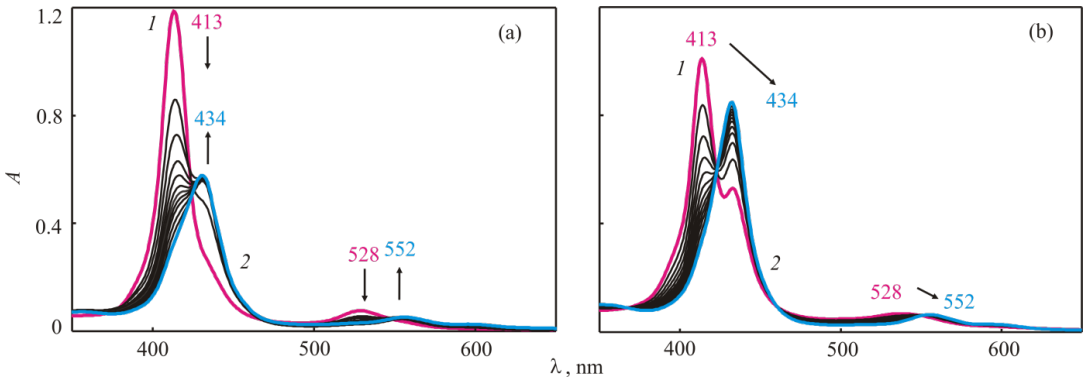

Figure 4. The UV-Vis spectra of CoT(4-CF_3Ph)P ($C = 5.12 \cdot 10^{-6}$ mol·L^{-1}) with the addition of Im: $C_{Im} = 7.24 \cdot 10^{-5}$ mol·L^{-1} at τ = 0 (*1*) and after 4 h (*2*) (a) and $C_{Im} = 3.33 \cdot 10^{-3}$ mol·L^{-1} at τ = 0 (*1*) and after 1 h (*2*) (b). The remaining lines correspond to intermediate points in time.

Table 1. The parameters for the bases in the reactions of the coordination on CoT(4-CF_3Ph)P in toluene: equilibrium constants and coordination rates (K_n and k_2), the number of reacting molecules (m), the reaction order (n), the relative optical response (A_{opt}) and the minimum detection limit (C_{min}).

MP – a base	K_n, L·mol^{-1}	*m*	k_2, L·mol^{-1}·s^{-1} k_{2-}, s^{-1}	*n*	A_{opt}	C_{min}, mol·L^{-1}
CoT(4-CF_3Ph)P – Py	$3.16 \cdot 10^3$ $1.53 \cdot 10^3$	0.88 0.98	$5.61 \cdot 10^{-4}$ $3.67 \cdot 10^{-7}$	0.73	0.18	0.00119
CoT(4-CF_3Ph)P – Im	$1.12 \cdot 10^4$ $4.28 \cdot 10^3$	1.06 0.87	1.033 $2.41 \cdot 10^{-4}$	0.72	0.21	0.000145
CoTPP – Py[44]	$7.94 \cdot 10^2$					
CoT(CF_3Ph)P – PyC_{60}[32]	$(5.89 \pm 1.50) \cdot 10^4$ $(7.40 \pm 1.66) \cdot 10^5$	1.24 1.25	78 ± 2	0.71		
CoTPP – PyC_{60}[45]	$(5.43 \pm 1.21) \cdot 10^4$ $(8.69 \pm 1.39) \cdot 10^4$	0.83 1.19	9.57 ± 0.15	0.80		

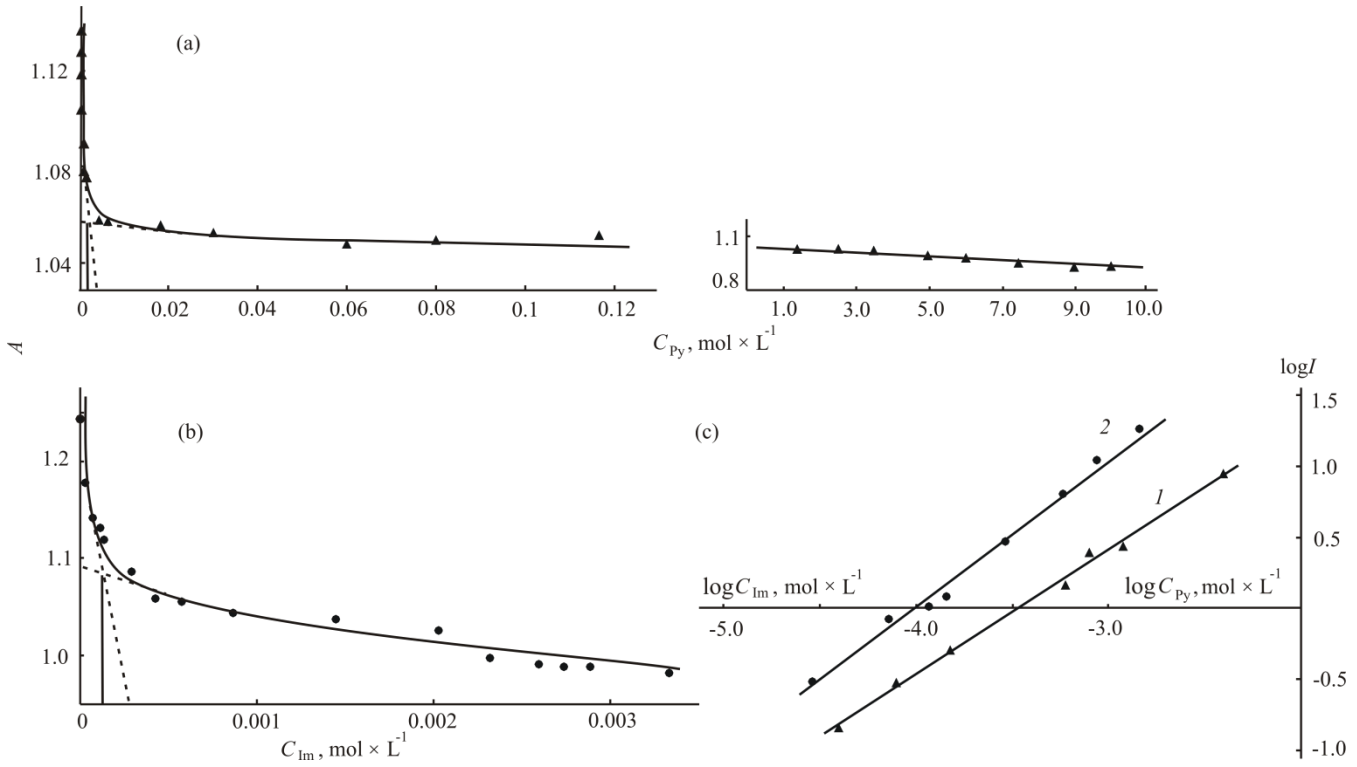

Figure 5. The curves of the CoT(4-CF_3Ph)P spectrophotometric titration in toluene at 298 K and τ = 0 with Py, $C_{MP} = 4.95 \cdot 10^{-6}$ mol·L^{-1}, C_{Py} 0 – 9.93 mol·L^{-1}, (a) and with Im, $C_{MP} = 5.12 \cdot 10^{-6}$ mol·L^{-1}, C_{Im} 0 - $3.33 \cdot 10^{-3}$ mol·L^{-1} (b) and the corresponding dependence $\log((A_i - A_o)/(A_\infty - A_i))$ for (*1*) Py and (*2*) Im, respectively (c). R^2 is equal to 0.9953 (*1*) and 0.9913 (*2*).

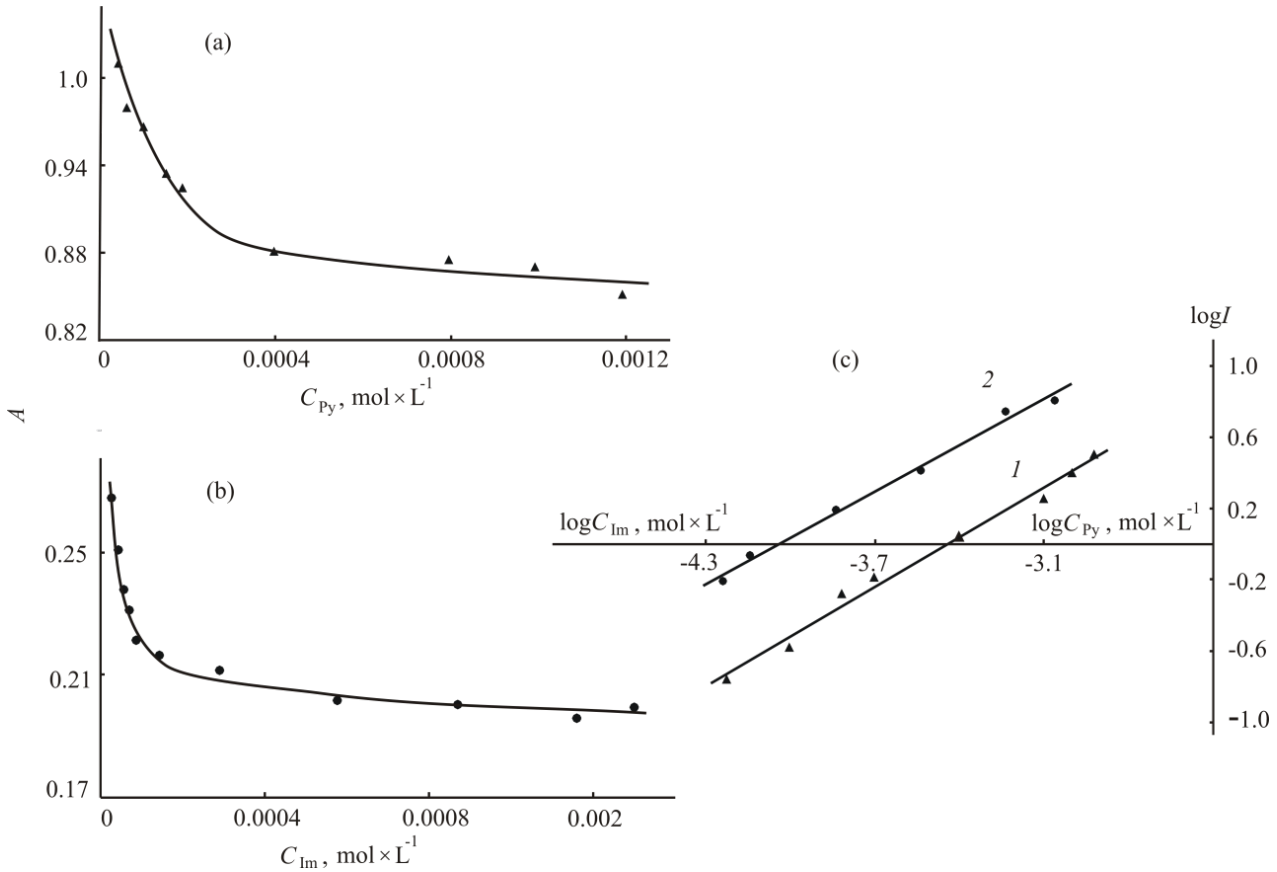

Figure 6. The curves of the CoT(4-CF_3Ph)P spectrophotometric titration in toluene at 298 K and τ = ∞ with Py, $C_{MP} = 4.95 \cdot 10^{-6}$ mol·L^{-1}, C_{Py} 0 – 9.93 mol·L^{-1}, (a) and with Im $C_{MP} = 5.12 \cdot 10^{-6}$, C_{Im} 0 - $3.33 \cdot 10^{-3}$ mol·L^{-1} (b) and the corresponding dependences $\log((A_i - A_o)/(A_\infty - A_i))$ for (*1*) Py and (*2*) Im, respectively (c). R^2 is equal to 0.9839 (*1*) and 0.9923 (*2*).

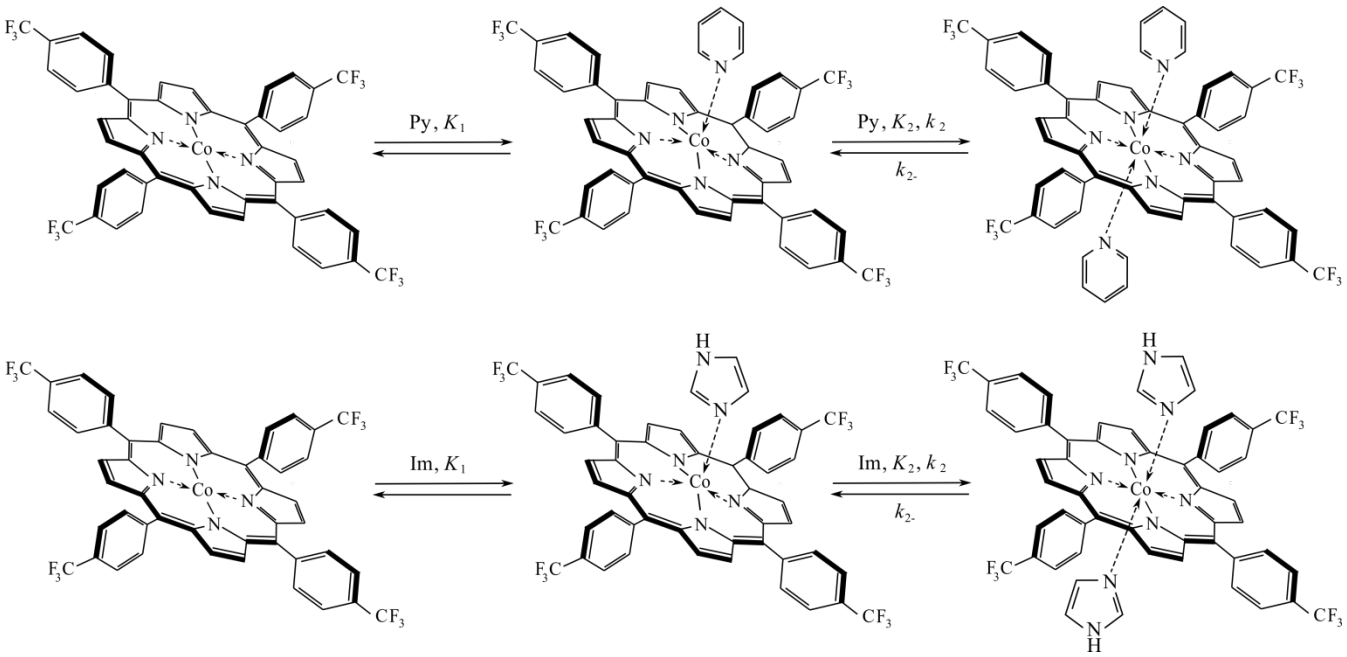

Scheme 1. Scheme of the simple reactions during the interaction of CoT(4-CF3Ph)P with a base.

Taking into account the statistical data on the number of Co^{II} complexes with coordination numbers 5 and 6, the structure of which was established using X-ray diffraction[49], the above data make it possible to write down the sequence of two-way simple reactions of CoT(4-CF_3Ph)P with a base (Scheme 1).

The axial complexation of CoT(4-CF_3Ph)P with the base molecules is reflected in its 1H NMR spectrum in the shift of the proton signals and the appearance of signals of a coordinated base. The singlet broadened proton signals of the macrocyclic ligand in the spectrum of CoT(4-CF_3Ph)P in a weak field are recorded, indicating the paramagnetic nature of the porphyrin complex (Figure 7). The pronounced upfield shifts of the macrocycle β-proton signals as well as the phenyl o- and m-proton signals in the ^{1}H NMR spectrum of hexacoordination Py and Im complexes from 15.71 ppm, 13.10 ppm, 10.18 ppm (CoT(4-CF_3Ph)P) to, respectively, 14.12 ppm, 11.01 ppm, 9.43 ppm and 8.69 ppm, 8.37 ppm, 7.63 ppm are observed. The upfield signal shifts of the 4-CF_3Ph protons is especially significant in the case of axial imidazole complex, *i.e.* complex with a stronger base. The resonance of protons of coordinated bases is observed in stronger fields relative to similar signals of the free bases only for protons located closest to the coordination center. Well-resolved H_o and $H_{Im(2)}$ proton signals of the coordinated bases were detected at 7.95 ppm and 7.46 ppm for Py and Im complexes, respectively, while these are 8.62 ppm and 7.70 ppm for the corresponding free bases.[50,51] Thus, ^{1}H NMR studies confirm not only the chemical structure of hexacoordinated Co(Py)$_2$T(4-CF_3Ph)P and Co(Im)$_2$T(4-CF_3Ph)P but also their paramagnetic nature. It was determined in[21] that the ground states of fully fluorinated complexes (L)$_2$CoTPPF$_{28}$ with medium-strength ligands Py, 1-MeIm, Im are identified as high-spin $4E_g$, which is consistent of the experimental ^{19}F NMR measurements.

The MS method (MALDI-TOF) made it possible to detect in the mass spectra of Py/Im axial CoT(4-CF_3Ph)P complexes (Figure 8) molecular ions that lack two base molecules (Experimental). However, in the ^{1}H NMR spectra of Co(Py)$_2$T(4-CF_3Ph)P and Co(Im)$_2$T(4-CF_3Ph)P there are no signals from the CoT(4-CF_3Ph)P protons (Figure 7). Therefore, it is obvious that the dissociation of Co-N bonds with two base molecules occurs under the conditions of recording mass spectra.

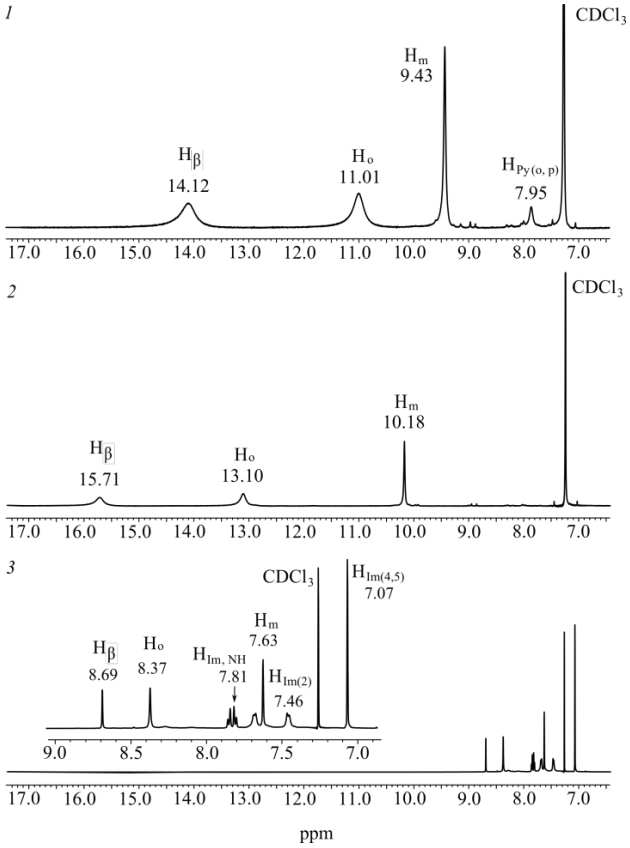

Figure 7. The ^{1}H NMR spectra of Co(Py)$_2$T(4-CF_3Ph)P (1), CoT(4-CF_3Ph)P (2), Co(Im)$_2$T(4-CF_3Ph)P (3) in $CDCl_3$. The signals at 7.84 ppm and 7.69 ppm correspond to uncoordinated Im specially added in the Co(Im)$_2$T(4-CF_3Ph)P solution.

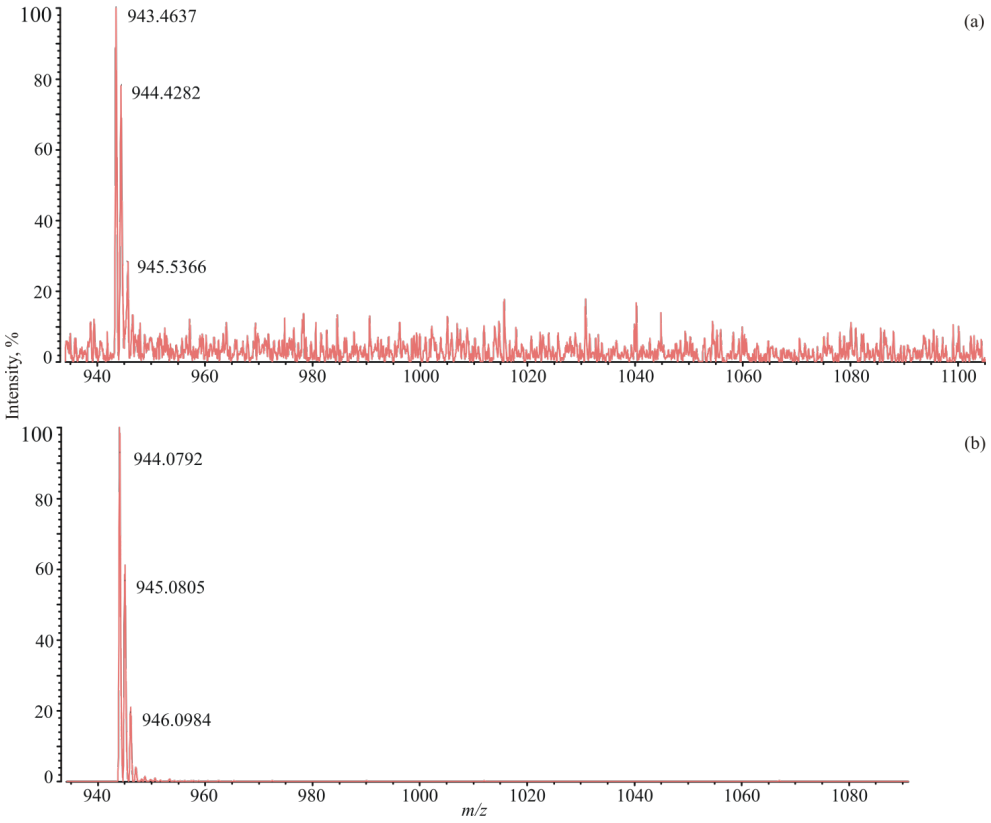

Figure 8. The mass spectrum of $Co(Py)_2T(4\text{-}CF_3Ph)P$ (a) and $Co(Im)_2T(4\text{-}CF_3Ph)P$ (b). The DHB matrix.

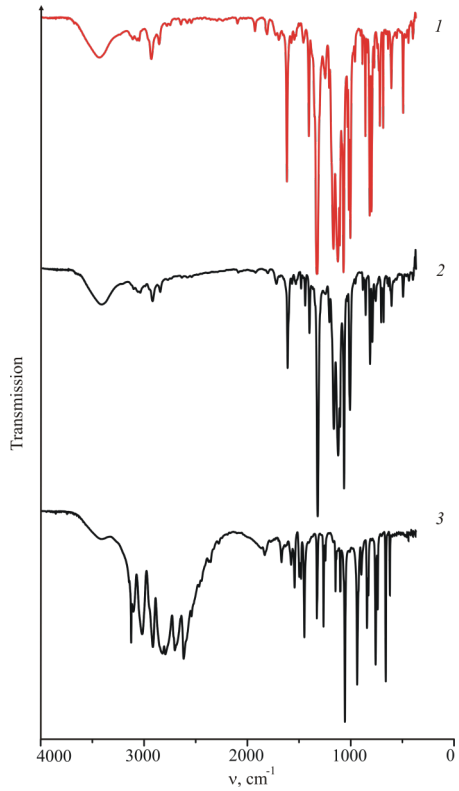

Figure 9. The IR spectra of $CoT(4\text{-}CF_3Ph)P$ (*1*), $Co(Py)_2T(4\text{-}CF_3Ph)P$ (*2*) and $Co(Im)_2T(4\text{-}CF_3Ph)P$ (*3*) in the tablets with KBr.

The $Co(Im)_2T(4\text{-}CF_3Ph)P$ IR spectrum (Figure 9) undergoes significant changes in the high frequency region compared with $CoT(4\text{-}CF_3Ph)P$. There is the significant increase in the relative intensity of the benzene ring ν(C–H) stretching vibration peak, its broadening and the low-frequency shift to 3016 cm^{-1} relative to the similar absorption of $CoT(4\text{-}CF_3Ph)P$. This signal in the $Co(Py)_2T(4\text{-}CF_3Ph)P$ spectrum is weak and slightly shifted. Intensity of the C=N vibration signal of the pyrrole rings increases from $CoT(4\text{-}CF_3Ph)P$ to $Co(Im)_2T(4\text{-}CF_3Ph)P$. The very strong well-resolved δ(C–H) signals of benzene rings appear at 1068 $cm^{-1}$and 1056 cm^{-1} in the "fingerprint" region in the $Co(Py)_2T(4\text{-}CF_3Ph)P$ and $Co(Im)_2T(4\text{-}CF_3Ph)P$ spectra. They are shifted to the low-frequency region of the spectrum. γ(C–H) vibrations of benzene rings are quite strong and shifted to high frequencies. The Co–N bonds were detected by absorption at 442 cm^{-1}, 438 cm^{-1}, and 441 cm^{-1} (Figure 9, *1*, *2*, *3,* respectively). New signals corresponding to vibrations of Py and Im coordinated appear at 694 cm^{-1}, 762 cm^{-1}, 1486 cm^{-1} and 897 cm^{-1}, 1263 cm^{-1}, 1832 cm^{-1}, respectively.

Thus, the totality of spectral data confirms the chemical nature of the reaction products in Scheme 1. As can be seen from the data in Table 1, the coordination equilibrium constant of both the first and the second Im molecule is several times higher than that for Py. Wherein, the K_1 constant of Py to $CoT(4\text{-}CF_3Ph)P$ coordination is four times higher than the corresponding value for unsubstituted CoTPP. Using the currently available data on the equilibrium constants of the one N-base molecule coordination by cobalt(II) porphyrin complexes, we can give a stability series of the corresponding pentacoordination complex in dichloromethane (a) and toluene (b):

$Co(MeIm)(TPPF_{28})^a$ $(6.31\cdot10^6)$[48] > $Co(Py)(TPPF_{28})^a$ $(7.94\cdot10^5)$[48] > $Co(Py)(TPPF_8)^a$ $(1.99\cdot10^4)$[48] > $Co(Im)T(4\text{-}CF_3Ph)P$ $(1.12\cdot10^4)^b$ (Table 1) > $Co(Py)T(4\text{-}CF_3Ph)P$

$(3.16\cdot10^3)^b$ (Table 1) > Co(MeIm)T(*o*-OCH_3)PP $(2.34\cdot10^3)^a$ [46] > Co(Py)TPP $(7.94\cdot10^2)^a$ [44] > Co(Py)T(*o*-OCH_3)PP $(4.79\cdot10^2)^a$ [46] > (Py)CoP $(3.56\cdot10^2)^a$ [36] (P is the 2,3,7,8,12,18-hexamethyl-13,17-diethyl-5-(2-pyridy-l)porphyrin dianion).

It can be seen that the higher the basicity of the axial ligand and the electron-withdrawing properties of *meso*-substituents in the macrocycle, the higher is the stability of pentacoordination Co^{II} complexes without steric hindrance. As for the hexacoordination complexes $Co(L)_2T(4\text{-}CF_3Ph)P$, Im derivatives are also formed at higher rates. It becomes clear from this, why $CoT(4\text{-}CF_3Ph)P$ demonstrates more acceptable chemosensory A_{opt} and C_{min} parameters in relation to Im.

The pyridyl group has already been used as the bridge between $CoT(4\text{-}CF_3Ph)P$ and N-methyl-substituted fullero-[60]pyrrolidine PyC_{60} (Table 1). $Co(PyC_{60})T(CF_3Ph)P$ is the donor-acceptor system with the fast intramolecular photoinduced electron transfer[32]. The formation constants of penta- and hexacoordination fullerene-containing complexes are orders of magnitude higher compared to Py (Table 1). Despite the lack of similar data for Im-containing complexes, it is possible to predict from the data presented above the higher coordination activity of Im-substituted fullero[60]pyrrolidine ImC_{60} when creating the donor-acceptor systems with $CoT(4\text{-}CF_3Ph)P$. The correctness of this prediction is supported by the data published for the Py[52] and Im complexes[35] with CoPc(3.5-di-^{t}BuPhO)$_8$ and (AcO)MnPc(3.5-di-^{t}BuPhO)$_8$.

Conclusions

(5,10,15,20-Tetra(4-trifluoromethylphenyl)porphinato)cobalt(II), $CoT(4\text{-}CF_3Ph)P$, interacts with the Py and Im molecules to form penta- and hexacoordination 1:1 and 1:2 complexes according to the data of UV-visible, IR, ^{1}H NMR and MS (MALDI-TOF) spectrometry. The coordination reaction in toluene occurs in two stages, but not in a concentration field, but in a time field, as a quickly and slowly established equilibrium with constants K_1, K_2 equal to $3.16\cdot10^3$ L·mol^{-1}, $1.53\cdot10^3$ L·mol^{-1} and $1.12\cdot10^4$ L·mol^{-1}, $4.28\cdot10^3$ L·mol^{-1} for Py and Im respectively. Reactions in the forward direction of the slow-establishing equilibrium are approximately three orders of a magnitude faster compared to the reverse reaction for both bases, while reactions with Im are faster. The stability of pentacoordination Co^{II} complexes without steric hindrance, according to both this work and available data for other porphyrin Co complexes, is higher, the higher the axial ligand basicity and the electron-withdrawing properties of the meso-substituents in the macrocycle. The higher coordination activity of Im-substituted fullero[60]pyrrolidine when creating the donor-acceptor systems with $CoT(4\text{-}CF_3Ph)P$ is predicted in order to obtain the donor-acceptor pairs with the property of the photoinduced charge separation and the formation of a radical salt.

Acknowledgements. The work was performed within the framework of the Program of State Academies of Sciences for 2023 - 2025, Topic 122040500043-7. That was carried out with the help of the center of the scientific equipment collective use «The upper Volga region center of physic-chemical research».

References

1. Lomova T.N. *Axially Coordinated Metalloporphyrins in Science and Applications*. Moscow: Krasand, **2019** [Ломова Т.Н. *Аксиально координированные металлопорфирины в науке и практике*. М.: Красанд, **2019**. 704 с.] https://www.rfbr.ru/rffi/ru/books/o_2087172.
2. Hong Y.H., Lee Y.-M., Nam W., Fukuzumi S. *J. Porphyrins Phthalocyanines* **2023**, *27*, 11–22. DOI: 10.1142/S1088424622300075.
3. Abdinejad M., Seifitokaldani A., Dao C., Sargent E.H., Zhang X., Kraatz H.B. *ACS Appl. Energy Mater*. **2019**, *2*, 1330−1335. DOI:10.1021/acsaem.8b01900.
4. Lomova T.N., Motorina E.V., Klyuev M.V. *Macroheterocycles*, **2013**, *6*, 327–333. DOI: 10.6060/mhc130644l.
5. Basova T.V., Belykh D.V., Vashurin A.S., Klyamer D.D., Koifman O.I., Krasnov P.O., Lomova T.N., Loukhina I.V., Motorina E.V., Pakhomov G.L., Polyakov M.S., Semeikin A.S., Stuzhin P.A., Sukhikh A.S., Travkin V.V. *J. Struct. Chem.* **2023**, *64*, 766–852. DOI: 10.1134/S0022476623050037.
6. Motorina E.V., Klimova I.A., Bichan N.G., Lomova T.N. *Russ. J. Inorg. Chem.* **2022**, *67*, 1993–2002. DOI: 10.1134/S0036023622601088.
7. Lomova T.N. *Macroheterocycles* **2021**, *14*, 299–311. DOI: 10.6060/mhc224201l.
8. Guo M., Zhang J., Zhang L., Lee Y.-M., Fukuzumi S., Nam W. *J. Am. Chem. Soc*, **2021**, *143*, 18559−18570. DOI: 10.1021/jacs.1c08198.
9. Matsuda Y., Murakami Y. *Coord. Chem. Rev*. **1988**, *92*, 157–192. DOI: 10.1016/0010-8545(88)85008-2.
10. Klyamer D., Sukhikh A., Bonegardt D., Krasnov P., Popovetskiy P., Basova T. *Micromachines* **2023**, *14*, 1773–1792. DOI: 10.3390/mi14091773.
11. *Design and Applications of Nanomaterials for Sensors* (Seminario J.M., Ed.), Springer: Dordrecht, Heidelberg, London, New York. **2014**. DOI: 10.1007/978-94-017-8848-9.
12. Pattam H.K., Jadhav A.B., Cheran A., Marydasan B., Kumar J. *J. Phys. Chem. C* **2023**, *127*, 17584−17591. DOI: 10.1021/acs.jpcc.3c03543.
13. Nierengarten J.-F. *J. Porphyrins Phthalocyanines* **2023**, *27*, 1253–1262. DOI: 10.1142/S1088424623500803.
14. Liu Q., Sun Q., Shen J., Zhang Y., Li H., Yu S., Chen Y., Li X., Jiang J. *J. Porphyrins Phthalocyanines* **2023**, *27*, 1119–1125. DOI: 10.1142/S1088424623500426.
15. Donga X., Lin W., Wang S., Zhang H., Zhang Z., Xie C., Li S., *J. Porphyrins Phthalocyanines* **2023**, *27,* 1103–1107. DOI: 10.1142/S1088424623500372.
16. Dorovskikh S.I., Klyamer D.D., Fedorenko A.D., Morozova N.B., Basova T.V. *Sensors* **2022**, *22*, 5780–5799. DOI: 10.3390/s22155780.
17. Shepeleva I.I., Birin K.P., Polivanovskaia D.A., Martynov A.G., Shokurov A.V., Tsivadze A.Y.; Selektor, S.L., Gorbunova Y.G. *Chemosensors* **2023**, *11*, 43–62. DOI: 10.3390/chemosensors11010043.
18. Terazono Y., Patrick B.O., Dolphin D.H. *Inorg. Chim. Acta* **2003**, *346*, 265−269.
19. Yang J., Huang P. *Chem. Mater*. **2000**, *12*, 2693–2697. DOI: 10.1021/cm0010506.
20. Beigulenko D.V., Shepeta N.Yu., Kochetkov K.A., Gelperina S.E. *Macroheterocycles* **2022**, *15*, 6−17. DOI: 10.6060/mhc224244k.
21. Liao M.-S., Watts J.D., Huang M.-J.. *J. Phys. Chem. A* **2005**, *109*, 11996−12005. DOI: 10.1021/jp058212b.
22. Beiler A.M., Khusnutdinova D., Wadsworth B.L., Moore G.F. *Inorg. Chem*. **2017**, *56*, 12178−12185. DOI: 10.1021/acs.inorgchem.7b01509.

23. Ke X., Kumar R., Sankar M., Kadish K.M. *Inorg. Chem*. **2018**, *57*, 1490−1503. DOI: 10.1021/acs.inorgchem.7b02856.
24. Lomova T.N., Motorina E.V., Bichan N.G.. *J. Porphyrins Phthalocyanines* **2022**, *26*, 485–494. DOI: 10.1142/S1088424622500365.
25. Ovchenkova E.N., Bichan N.G., Lomova T.N. *Russ. J. Inorg. Chem.* **2018**, *63*(3), 391–399. DOI: 10.1134/S0036023618030178.
26. Ovchenkova E.N., Elkhovikova A.A., Lomova T.N. *Russ. J. Inorg. Chem*. **2024**, *69*(1), 26–32. DOI: 10.1134/S0036023623602726.
27. Motorina E.V., Lomova T.N. *Russ. J. Inorg. Chem.* **2010**, *55*, 727–733. DOI: 10.1134/S0036023610050116.
28. Motorina E.V., Lomova T.N. *Russ. J. Gen. Chem.*, **2010**, *80*, 842–848. DOI: 10.1134/S1070363210040274.
29. Bichan N.G., Ovchenkova E.N., Lomova T.N. *Russ. J. Phys. Chem. A* **2019**, *93*, 703–709. DOI: 10.1134/S003602441904006X.
30. Motorina E.V., Lomova T.N., Mozhzhukhina E.G., Gruzdev M.S. *Russ. J. Inorg. Chem.* **2019**, *64*, 1538–1547. DOI: 10.1134/S0036023619120106.
31. Lomova T.N., Motorina E.V., Mozhzhukhina E.G., Gruzdev M.S. *J. Porphyrins Phthalocyanines* **2020**, *24*, 1224–1232, DOI: 10.1142/S1088424620500406.
32. Ovchenkova E.N., Motorina E.V., Bichan N.G., Gostev F.E., T.N. Lomova. *J. Organomet. Chem*, **2022**, *977*, 122458. DOI: 10.1016/j.jorganchem.2022.122458.
33. Bichan N.G., Mozgova V.A., Ovchenkova E.N., Gruzdev M.S., Lomova T.N. *Russ. J. Inorg. Chem*, **2023**, *68*, 825–832. DOI: 10.1134/S0036023623600892.
34. Ovchenkova E.N., Bichan N.G., Gruzdev M.S., Ksenofontov A.A., Lomova T.N., Gostev F.E., Shelaev I.V., Nadtochenko V.A. *New J. Chem.* **2021**, *45*, 9053–9065. DOI: 10.1039/d1nj00980j.
35. Ovchenkova E.N., Bichan N.G., Kudryakova N.O., Gruzdev M.S., Lomova T.N., Tsaturyan A.A., Gostev F.E., Shelaev I.V., Nadtochenko V.A. *J. Phys. Chem. C* **2020**, *124*, 4010–4023. DOI: 10.1021/acs.jpcc.9b11661.
36. Ovchenkova E.N., Bichan N.G., Semeikin A., Lomova T.N. *Macroheterocycles* **2018**, *11*, 79–84. DOI: 10.6060/mhc170301o.
37. Bichan N.G., Ovchenkova E.N., Lomova T.N. *Russ. J. Inorg. Chem.* **2018**, *63*, 1453–1460. DOI: 10.1134/S0036023618110037.
38. Timoschenko L.V., Sarycheva E.A. *Heterocyclic Compounds*. **2013**. 90 p. [Тимощенко Л.В., Сарычева Т.А. *Гетероциклические соединения: учебное пособие*. Томск: Изд-во Томского политехнического ун-та. **2013**. 90 с.].
39. Torshin I.Yu., Gromova O.A., Maiorova L.A. *Farmakoekonomika. Modern Pharmacoeconomics and Pharmaco-epidemiology* **2023**, *16*, 501–511. DOI: 10.17749/2070-4909/farmakoekonomika.2023.198.
40. Krasley A.T., Li E., Galeana J.M., Bulumulla C., Beyene A.G., Demirer G.S. *Chem. Rev.* **2024**, *124*, 3085–3185. DOI: 10.1021/acs.chemrev.3c00581.
41. Lomova T.N. In: *Theoretical and Experimental Methods of Solution Chemistry*. Moscow: Prospekt Publishing House, **2011**. 688 p. [Ломова Т.Н. В кн.: *Теоретические и экспериментальные методы химии растворов (Проблемы химии растворов)* (Цивадзе А.Ю., ред.), М.: Проспект, **2011**. 688 с., ISBN 978-5-392-02419.
42. Yurovskaya M.A., Kurkin A.V., Lukashev N.V. *Chemistry of Aromatic Heterocyclic Compounds*. Moscow. **2007**, 50 p. [Юровская М.А., Куркин А.В., Лукашев Н.В. *Химия ароматических гетероциклических соединений*, М.: МГУ, **2007**].
43. Mack J., Stillman M.J. *J. Porphyrins Phthalocyanines* **2001**, *5*, 67.
44. Kadish K.M., Bottomley L.A., Beroiz D. *Inorg. Chem*. **1978**, *17*, 1124–1129. DOI: 10.1021/ic50183a006.
45. Bichan N.G., Ovchenkova E.N., Mozgova V.A., Kudryakova N.O., Lomova T.N. *Russ. J. Inorg. Chem.* **2019**, *64,* 605–614. DOI: 10.1134/S00360 23619050024.
46. Walker F.A. *J. Am. Chem. Soc.* **1973**, *95*, 1150.
47. Lin X.Q., Boisselier Cocolios B., Kadish K.M. *Inorg. Chem.* **1986**, *25*, 3242–3248. DOI: 10.1021/ic00238a030.
48. Smirnov V.V., Woller E.K., DiMagno S.G. *Inorg. Chem.* **1998**, *37*, 4971–4978. DOI: 10.1021/ic980156o.
49. Solov'ev V.P., Stuklova M.S., Koltunova E.V., Kochanova N.N. *Coord. Chem*, **2003**, *29*(9), 711–720.
50. Fulmer G.R., Miller Alexander J.M., Sherden N.H., Gottlieb H.E., Nudelman A., Stoltz B. M., Bercaw J.E., Goldberg K.I. *Organometallics* **2010**, *29*, 2176–2179. DOI: 10.1021/om100106e.
51. Gordon A.J., Ford R.A. The Chemist's Companion (engl. Transl.). Moscow: Mir, **1976**. [Гордон А., Форд Р. *Спутник химика*. М.: Мир, **1976**].
52. Bichan N.G., Ovchenkova E.N., Kudryakova N.O., Lomova T.N. *J. Mol. Liq*. **2019**, *280*, 382–388. DOI: 10.1016/j.molliq.2019.01.025.

Received 15.04.2024
Accepted 23.11.2024